Inhibition of Copper Corrosion by Ethanolamine in 100 ppm NaCl

Abderrahim, Karima; Abderrahmane, Sihem*[+]

Laboratoire d'Ingénierie Des Surfaces (L. I. S.)-Université Badji Mokhtar
B.P. 12 - 23000 Annaba, ALGERIE

Millet, Jean-Pierre

INSA-Lyon, MATEIS CNRS UMR5510,F-69621 Villeurbanne, FRANCE

ABSTRACT: *We study copper corrosion inhibition by ethanolamine (ETA) with (0, 0.2 ,0.3,0.4,0.5) vol.% concentrations in 100 ppm NaCl solution. This work is carried out by potentiodynamic measurements and Electrochemical Impedance Spectroscopy (EIS). The substrates' surface morphologies are examined by Scanning Electron Microscopy (SEM). ETA is characterized by NMR spectra of ETA ^{1}H and ^{13}C and Fourier Transform InfraRed Spectroscopy (FT-IR).Quantum chemical calculation (DFT) is conducted to correlate the adsorption mechanism with ETA molecule structure. The results show that ETA acts as a mixed inhibitor; so at 0.4 vol. %, the current density (i) and the polarization resistance (Rp) are respectively 0.8µA/cm² and 28.62 Ω.cm² with 99.78% corresponding efficiency . ETA adsorption obeys to Langmuir isotherm and takes place on copper surface through chemical and physical mixed-type adsorption.*

KEYWORDS: *Copper Corrosion; Corrosion Inhibitor; ETA; EIS; Polarization.*

INTRODUCTION

Copper is a widely used metal because of its excellent electrical and thermal conductivities combined with good mechanical work-ability [1]. It is also known for its good corrosion resistance in both water and deaerated non-oxidizing acid solutions. However, copper may undergo rapid attack in complexing agents presence as for example with Cl^- ions which form soluble chloro-complexes $CuCl_j^{(2-j)-}$ [where j=1 to 4].

According to J. Crousier et al. [2] the complex $CuCl_2^-$ could be formed either in two steps [reactions (1) and (2)] or directly [reaction (3)] as below:

$$Cu + Cl^- \leftrightarrow CuCl_{ads} + e^- \quad (1)$$

$$CuCl_{ads} + Cl^- \leftrightarrow CuCl_2^- \quad (2)$$

$$Cu + 2Cl^- \leftrightarrow CuCl_2^- + e^- \text{ (Slow step)} \quad (3)$$

Therefore, the anodic dissolution rate is closely related to $CuCl_2$ diffusion rate in the solution. Whereas, minimal amounts of chloride concentration CuCl can be formed in the initial step, then the dissolution proceeding takes place in the $CuCl^-_2$ form. On metal surface, even the presence of insoluble products cannot prevent the oxygen reduction [3]. An interesting method to inhibit copper

* *To whom correspondence should be addressed.*
+ E-mail: abderrahmanesihem@yahoo.fr
1021-9986/2016/4/89 10/$/6.00

corrosion which is the use of organic inhibitors and compounds containing polar groups as nitrogen, sulfur and oxygen [4, 5] . Some of them can be produced at low cost with high purity and they are fully soluble in aqueous medium.

In the present work, we test ethanolamine corrosion inhibitor that contains $–NH_2$ and –OH groups (Fig. 1). The copper corrosion inhibition by ETA is carried out by potentiodynamic and electrochemical impedance spectroscopy methods in 100 ppm NaCl solution without and with ETA at various concentrations (0, 0.2, 0.3, 0.4, 0.5) vol. %.

EXPERIMENTAL SECTION

The copper composition obtained by ICP-MS (Inductively Coupled Plasma- Mass Spectrometry) is shown in Table 1.

The experimental device used for plotting polarization curves and electrochemical impedance is the potentiostat / galvanostat / ZRA Gamry Reference 1000 assisted with computer and related to standard three-electrode cell. The reference is Saturated Calomel Electrode (SCE) with E = 0.241 V vs SHE, the counter electrode is platinum and copper as the working electrode. The latter has a circular section of $1cm^2$ that is polished mechanically with abrasive SiC paper up to grade 4000, then finished with diamond paste (1µm).In order to allow electric connection, a copper wire is welded onto the opposed face of the working surface. Except this latter, the whole sample is embedded in an epoxy resin.

The tests are performed without and with ETA, in 100 ppm NaCl aerated aqueous solution, at various concentrations (0, 0.2, 0.3, 0.4, 0.5) vol.%. The potentiodynamic curves are plotted in potentials' range −1200 to +600 mV vs SCE with 1 mV/s scan rate. Electrochemical Impedance Spectroscopy (EIS) measurements are carried out in the frequency range 100 kHz-10 mHz at the open circuit potential using the amplitude 10 mV. Transfer resistance R_{ct} and electrical double layer capacitance C_{dl} are deduced from Nyquist diagrams and the equivalent circuit is determined with Z-view software. All polarization experiments are performed in 100 ppm NaCl at 25^0C, after 2 hours immersion time. The test solution volume for each experiment is maintained at 200 mL. The substrates' surface morphologies are examined by scanning electron microscopy (SEM). ETA inhibitor characterization is carried out by NMR spectra (^{1}H and ^{13}C) and Fourier transforms infrared spectroscopy (FT-IR). Quantum chemical calculation (DFT) is used to correlate the adsorption mechanism with ETA molecule structure.

Table 1: copper chemical composition.

Elements	M (mass %) . 10^{-3}
Cu	99 960
Si	7
P	21
Ti	0.2
V	0.2
Mn	2.5
Sb	0.5
Co	0.1
Ni	3.1
Nb	1.8
Mo	1.0
Sn	2.9

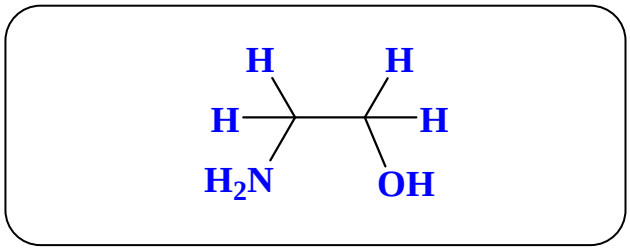

Fig. 1: ETA chemical structure.

RESULTS AND DISCUSSION

OCP recordings

Fig. 2 represents OCP curves versus time, in 100ppm NaCl with ETA at different concentrations (0,0.2,0.3,0.4,0.5) vol.% , that are obtained after two hours. At first, we observe that the OCP values are relatively stable from 1500s, then in presence of ETA, they are increasingly more negative compared to those obtained in its absence. We notice a significant difference (0.1V) in comparison to the OCP values obtained in the inhibited media, at the beginning, there is an increasing with the added amount until 0.4 vol.%, but then clearly fall down. As a result, the concentration 0.4 vol.% seems to be optimum.

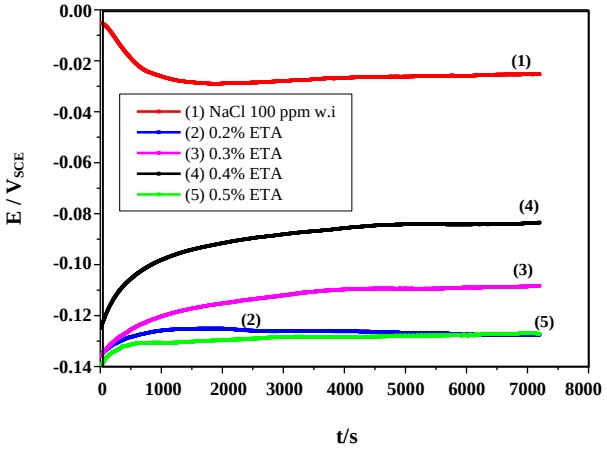

Fig. 2: OCP curves for copper in NaCl aqueous media with various inhibitor amounts.

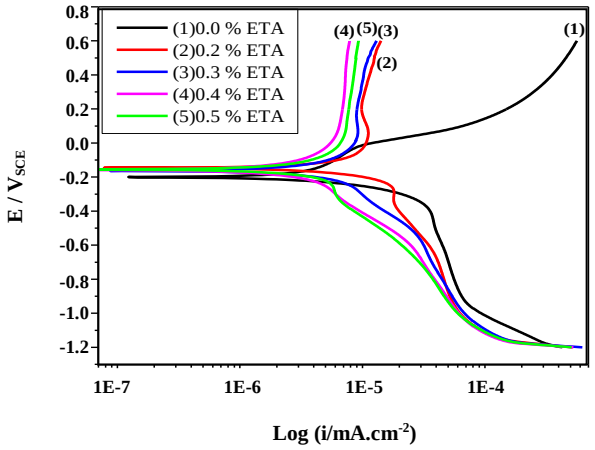

Fig. 3: Copper polarization curves with ETA concentrations (0,0.2,0.3,0.4,0.5) vol % in 100 ppm NaCl at 1mV/s scan rate.

Polarization measurements

Fig. 3 shows copper potentiodynamic polarization curves in 100 ppm NaCl without and with ETA at various concentrations.The cathodic corrosion reaction in an aerated NaCl solution is the oxygen reduction [6]:

$$O_2 + 2H_2O + 4e^- \leftrightarrow 4OH^- \quad (4)$$

Copper anodic dissolution process in NaCl solution which has been already reported [7-8], as follows:

$$Cu + Cl^- \rightarrow CuCl + e^- \quad (5)$$

$$CuCl + Cl^- \rightarrow CuCl_2^- \quad (6)$$

$$CuCl_2^- \rightarrow Cu^{2+} + 2Cl^- + e^- \quad (7)$$

The curves are obtained from −1200 to +600 mV vs SCE at 1 mV/s scan rate. The more negative value of the initial cathodic potential is chosen in order to clean the metallic surface by chemical reaction's reduction. On the curves, the cathodic parts present a more or less clear plateau corresponding to dissolved oxygen diffusion's reduction according to equation (4). The important cathodic polarization may explain the differences between the obtained OCP values and E_{corr}, i.e.$E_{i=0}$.

Among the anodic branches, the anodic curve increases significantly in inhibitor absence [Fig. 3 curve (1)]. But, in inhibitor presence, the effect is clearly apparent where the anodic plateau presence indicates a protective film formation which slows down corrosion. The anodic copper dissolution mechanisms can be decomposed in several steps [4-9], controlled by both copper electro dissolution and $CuCl^-_{2ads}$ diffusion in solution, equations (5-7).

Therefore, as previously observed above, we can consider that the most effective inhibitor concentration is 0.4 vol.%, since the anodic plateaus level diminishes, when ETA is added until this value, and increases at 0.5% addition. From these curves, Table 2 records all the electrochemical data: corrosion potential E_{corr} (mV vs SCE), corrosion current density i_{corr} ,cathodic *Bc* and anodic *Ba* Tafel slopes, polarization resistance Rp and corrosion rate v.

The corrosion rate (mm/y) is calculated using the Equation (8) [10].

$$v = kM\frac{i_{corr}}{2dA} \quad (8)$$

Where:

k :constant ;

M : copper molar mass (63.35 g/mol);

A: Avogadro number;

d : density (g/cm^3).

The inhibition efficiency (η) can also be calculated from equation (9) [11].

$$\eta(\%) = \frac{\left(i_{corr,o} - i_{corr,i}\right)}{i_{corr,o}} \times 100 \quad (9)$$

Where $i_{corr,0}$ and $i_{corr,i}$ are respectively the corrosion current densities of copper in 100 ppm NaCl without and with ETA.

Table 2: efficiencies calculated (η) and parameters derived from potentiodynamic polarization curves of copper in 100 ppm NaCl without and with ETA at different concentrations after 2h.

C (vol %)	E_{corr} mV vs SCE	i_{corr} (µA/cm²)	Ba (mV/dec)	Bc (mV/dec)	v (mm/y)	Rp (Ω cm²)	η (%)
0	-202.438	235.2	800.4	87.6	0.977	4.28	/
0.2	-166.109	4.2	726.1	425.0	0.344	20.64	98.34
0.3	-162.037	4.8	606.4	481.7	0.247	24.30	98.08
0.4	-259.945	0.8	587.9	420.4	0.066	28.62	99.78
0.5	-175.872	7.1	801.0	826.1	0.159	13.02	96.98

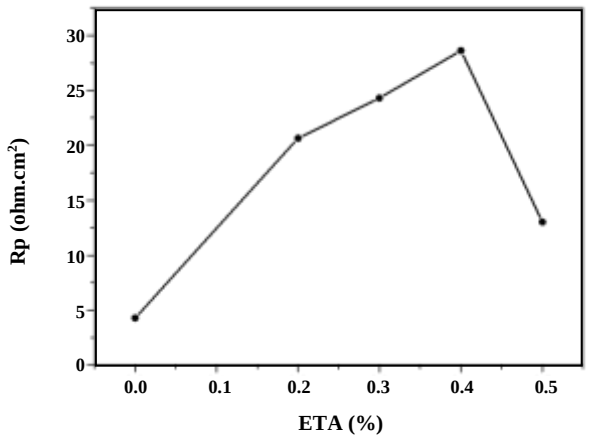

Fig. 4: Evolution of the polarization resistance according to ETA concentrations.

We note that the inhibitive efficiency increases in accordance with the inhibitor concentration at the maximum value (99.78 %) for 0.4 vol.% ETA and the polarization resistance Rp is closely related to ETA inhibitor concentration up to 0.4 vol.% when it increases till the maximum value (28.62 Ω.cm²). But Rp decreases beyond this concentration (Fig.4).

EIS measurements

Fig. 5 shows Nyquist and Bode diagrams obtained with copper in 100 ppm NaCl without and with ETA at concentrations (0, 0.2, 0.3, 0.4, 0.5) vol.%. All impedance spectra (Fig.5a) consist of one capacitive loop. The ETA concentration increasing leads to the increase of the semicircle diameter .In the case, where the center is under the real axis, can be attributed to roughness and heterogeneities of the solid surfaces.

The modulus and phase angle curves according to the frequencies are represented respectively in (Fig.5b) and (Fig.5c). The polarization resistance increases till maximum (148.222 Ω.cm²) for 0.4 vol.% . ETA inhibitor concentration and the phase angle plot (Fig.5c) consist in two time constants**.**

In Bode-phase plots, the impedance high frequency part and phase angle reflect heterogeneous surface layer behavior, while the low frequency contribution shows the kinetic response for the charge transfer reaction [12]. Electrochemical parameters derived from Fig. 4 are gathered in Table 3.

Fig. 6 represents the simulated equivalent circuit ,from Nyquist diagrams (Fig.5) ,where R_s,R_t, R_f **,** CPE_{dl} and CPE_f are respectively the electrolyte resistance, charge transfer resistance, film resistance , double layer constant phase element and film constant phase element**.**

When the inhibitor concentration increases, the R_t increases while CPE_{dl}decreases due to the reduction of the copper active surface [13].

The corrosion inhibitive efficiency is calculated from the charge transfer resistance according to the equation:

$$\eta(\%) = \left(1 - \frac{Rt'}{Rt}\right) \times 100 \qquad (10)$$

Where R_t' and R_t represent respectively the charge transfer resistance values in inhibitor presence and absence.

The efficiency increases versus inhibitor concentration then reaches a maximum value 97.80% at 0.4% vol. ETA with an error factor X^2= 6.99 E-4 **.** This result corroborates with the obtained one from polarization resistance measurements and corrosion current densities.

Cyclic voltammetry

Each cycle plot (Fig.7) is obtained by rate scanning (1 mV/S) from -1200 mV vs SCE to 600 mV vs SCE

Table 3: Inhibitive efficiencies (η) and parameters deduced from EIS curves of copper in 100 ppm NaCl without and with ETA at different concentrations.

C (vol %)	R_S (Ω cm²)	R_t (Ω cm²)	CPE_{dl} (µF/cm²)	R_f (Ω cm²)	CPE_f (µF/cm²)	n	η (%)	X^2 (error factor)
0	5.568	45	14.4	/	25.5	0.510	/	8.70 E-4
0.2	3.369	65	8.0	391	7.9	0.727	92.41	5.86 E-4
0.3	3.978	120	7.7	485	7.5	0.750	94.77	9.20 E-4
0.4	3.222	145	6.0	781	10.5	0.758	97.80	6.99 E-4
0.5	2.987	133	7.2	550	6.1	0.587	95.12	7.77 E-4

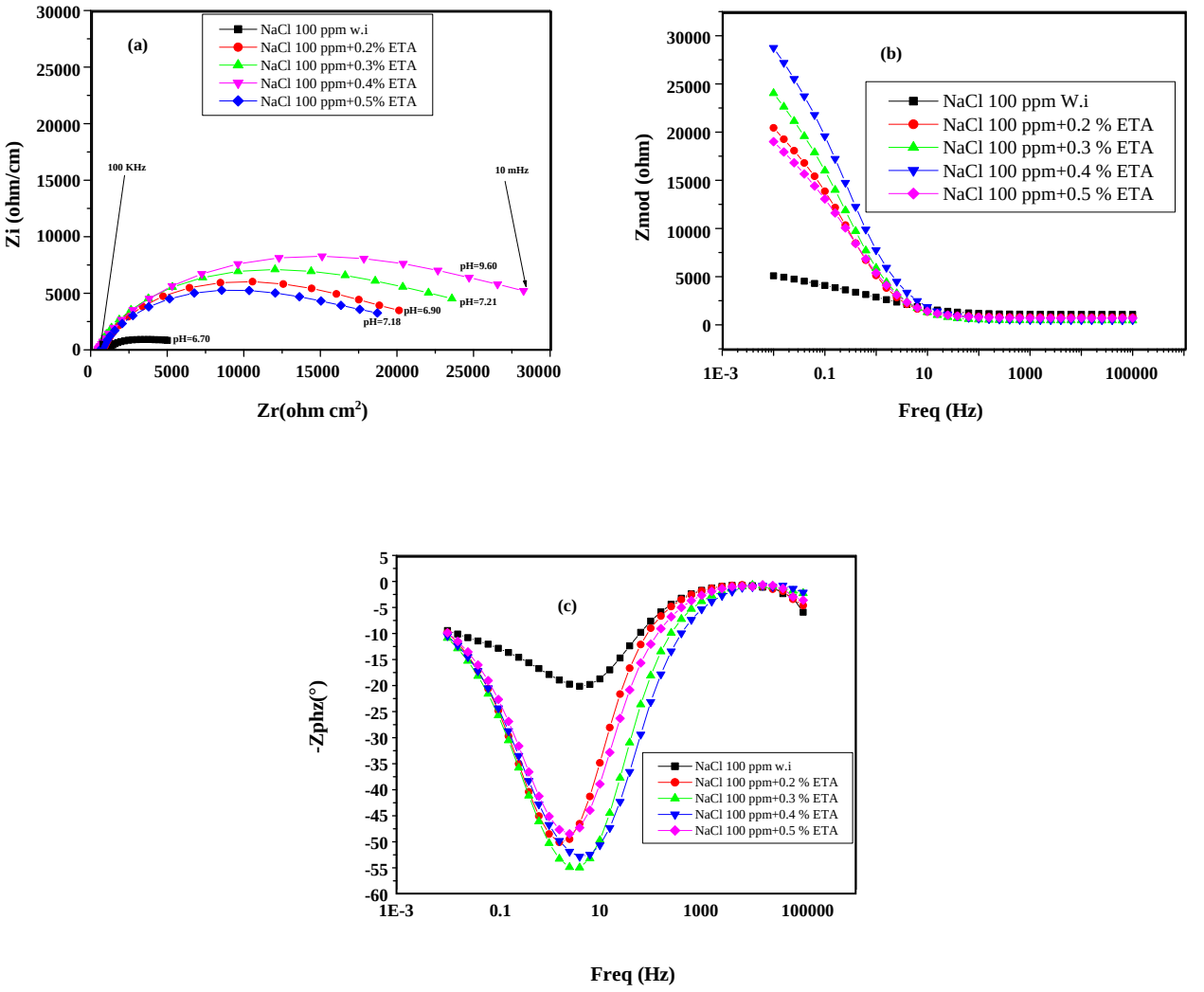

Fig. 4: Nyquist diagrams (a), Bode modulus (b) and phase angle (c) of copper in 100 ppm NaCl without and with ETA concentrations (0,0.2,0.3,0.4,0.5) vol %..

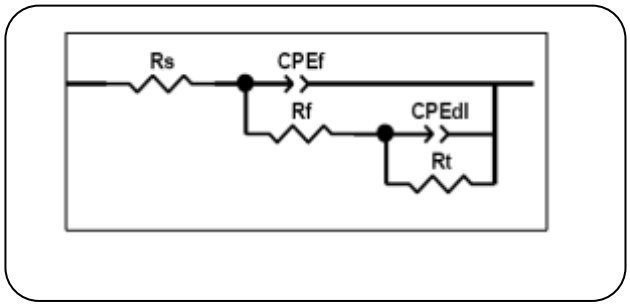

Fig. 6: Equivalent electrical circuit used to represent impedance data from Fig.5a Nyquist curves.

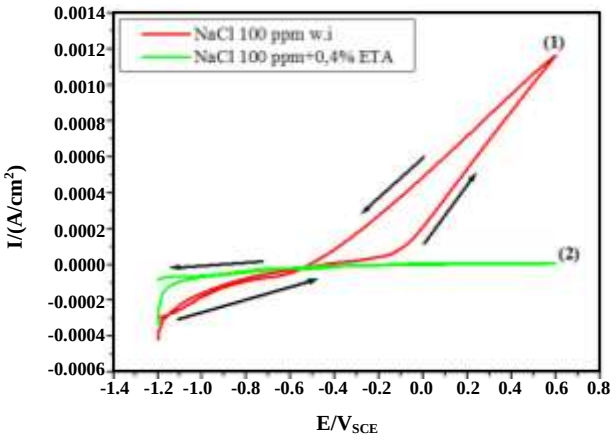

Fig. 7: Copper cyclic voltammogram in 100 ppm NaCl without and with 0.4 vol % ETA

leading to 0.1 mA/cm^2 current density then returns to the initial potential. In the solution without inhibitor, the resulted voltammogram is considered as a reference representing an active copper dissolution characterized by a large hysteresis. This behavior is explained by copper dissolution mechanism in chloride media [Cl^-] <1M [14]. In presence of H_2O, Cl^- and copper, copper hydroxide reflects a kinetic adsorption on the electrode surface. Similar results were obtained by Crousier et al. [2].

In the presence of inhibitor (0.4%vol.), the voltammogram goes and returns to the initial potential using the same way which reflects a perfect surface stability.

Adsorption isotherm

The adsorption of organic molecules at the metal/solution interface consists of the replacement of water molecules by organic molecules in aqueous solution according Equation (11) [15].

$$Org_{aq} + XH_2O_{ads} \leftrightarrow Org_{ads} + XH_2O_{aq} \quad (11)$$

Where:

Org_{aq}: organic molecules in the solution;

Org_{ads}: organic molecules adsorbed on the metal surface;

X: the number of water molecules replaced by the organic molecules.

Copper corrosion inhibition in 100 ppm NaCl with ETA is due to the molecular adsorption. This latter depends on organic compounds such as molecule charge distribution, metal nature; metal surface charge and aggressive medium type [16, 17] .The interaction between the adsorbed molecules of inhibitors and copper surface is explained by isotherms' adsorption [18].

The relationship between inhibition efficiency (ŋ %) and the coverage degree (θ) for different inhibitor concentrations is :

$$\eta\% = 100 \times \theta \quad (12)$$

Theoretical fitting of different isotherms adsorption is simulated and the correlation coefficients (R) are used. The most corresponding fit (R=0.999) is obtained by the Langmuir isotherm. The relation Langmuir isotherm is:

$$\theta = \frac{KC}{KC+1} \quad (13)$$

Where θ is the coverage degree on metal surface, *C* is the inhibitor concentration and K_{ads} is the equilibrium constant of adsorption process. This constant is related to the standard free energy of adsorption (ΔG°_{ads}) according to the following equation:

$$\Delta G^\circ_{ads} = -RT\ln\left(55.5K_{ads}\right) \quad (14)$$

Where R is the molar gas constant (8.314 (J/mol K) and T(K) is the absolute temperature.

The inhibitor adsorption obeys to Langmuir isotherm in accordance with the linear relationship (Fig. 8). The equation 14 is used to find the constant K as an intersection of straight line with the ordinate axis.

$$K_{ads} = \left(\frac{1}{55.5}\right)\exp\left(-\frac{\Delta G^\circ_{ads}}{RT}\right) \quad (15)$$

At 298 K, K_{ads}= 0.185×10^{4}M^{-1} and ΔG°_{ads} = -28.59 kJ/mol.

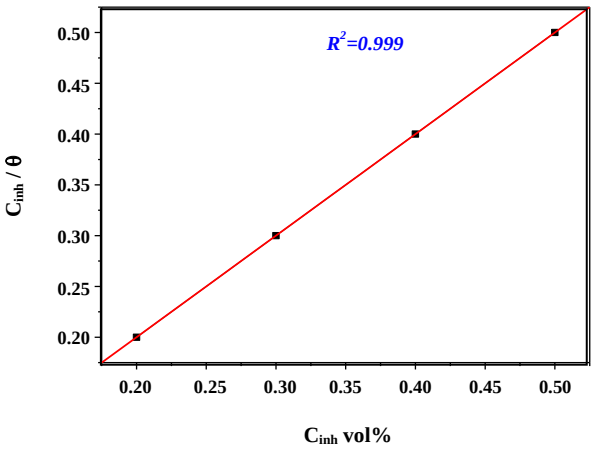

Fig. 8: Copper Langmuir adsorption in 100 ppm NaCl with ETA at different concentrations.

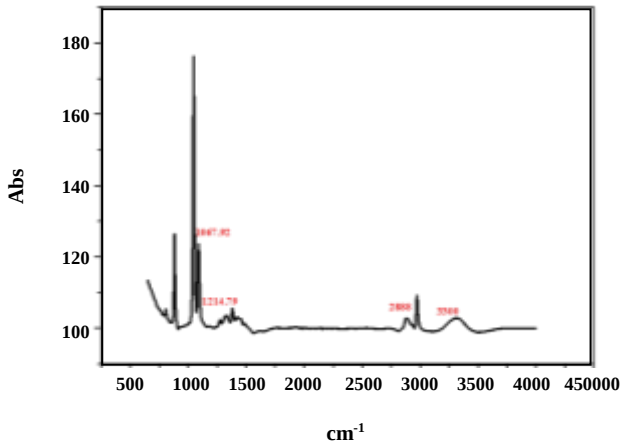

Fig. 9: FT-IR spectrum of ethanolamine.

The standard free enthalpy negative value indicates the strong interaction and stability of the adsorbed layer on copper surface. [19] and also the spontaneous adsorption of the ETA on the copper [20].

When $\Delta G^{\circ}_{ads} \leq$-20kJ/mol, the inhibitor molecules are physisorbed on metal surface. Whereas for $\Delta G^{\circ}_{ads} \geq$ -40 kJ/mol, the molecules are chemisorbed due to charge sharing or transfer to metal surface in order to form metal bond coordinate [21]. We conclude that the inhibitor ETA adsorption on copper surface takes place through mixed chemical and physical adsorption [22].

NMR spectra of ETA ^{1}H and ^{13}C

In ^{1}H NMR spectrum, two triplets appear at 2.54 ppm and 3.41 ppm, each signal is integrated to 2H corresponding to CH_2.

A signal at 4.10ppm is characteristic of the NH_2 function.

RMN ^{1}H (300MHz, DMSO): δ 2.54(t, 2H, *J*=6.0 Hz, CH_2-N), 3.41 (t, 2H, *J*=6.0 Hz, CH_2-O), 4.10 (s, 2H, NH_2) ppm.

In RMN ^{13}C spectrum, there is two peaks, the first at about 50 ppm and the second at 60 ppm. Both of them characterize two carbons ($2CH_2$) and the solvent peaks in which we have performed the analysis (in this spectrum the first peak shift's slightly to 57.5 ppm)

RMN ^{13}C (300MHz, DMSO): δ 57.5 (CH_2-N), 59.6 (CH_2-O) ppm.

Fourier transforms infrared spectroscopy (FT-IR)

Fig. 9 shows the FT-IR spectrum of ETA. The characteristic bands of ETA are assigned as follows:

sharp band at 3300cm^{-1} was due to N-H stretching vibration, 2888cm^{-1} was due to O-H stretching .

IR (KBr): 2888 (NH_2), 3300(OH) cm^{-1}.

From the interpretation of FT-IR spectra, we can conclude that the ETA inhibitor formula is: NH_2-CH_2-CH_2-OH.

Quantum chemical calculation (DFT)

To explain the adsorption, electronic parameters, associated at the interaction between the inhibitor molecules and the copper atoms, are computed using the standard 6-31G * basis and functional B3LYP. The values found are grouped in Table 4. In this case, E_{HOMO} is the energy of the highest occupied molecular orbital, E_{LUMO} is the energy of the lowest unoccupied atomic orbital and $\Delta E_{gap} = E_{HOMO} - E_{LUMO}$ is the gap energy.

The highest value E_{HOMO} (-5.0265 eV) indicates that the molecular orbitals tend to donate electrons to the atomic orbitals; these ones have an aptitude to accept according to the value E_{LUMO} (- 0.5369 eV) [23].

These frontier orbitals control the adsorbate-surface interaction. Small values ΔE gap (4.4896 eV), dipole moment (3.2334 Debye) as well as total energy (-1223.98 u.a.) indicate that the inhibitor molecules' adsorption on copper surface is stable and therefore effective. Optimized structure of the studied molecule obtained by

Table 4: calculated HOMO (eV), LUMO (eV), ΔE_{gap} (eV), dipole moment (debye) and total energy (u.a).

E_{HOMO} (eV)	E_{LUMO} (eV)	ΔE_{gap} (eV)	Dipole moment (Debye)	TE (u.a.)
-5.0265	- 0.5369	4.4896	3.2334	-1223.98

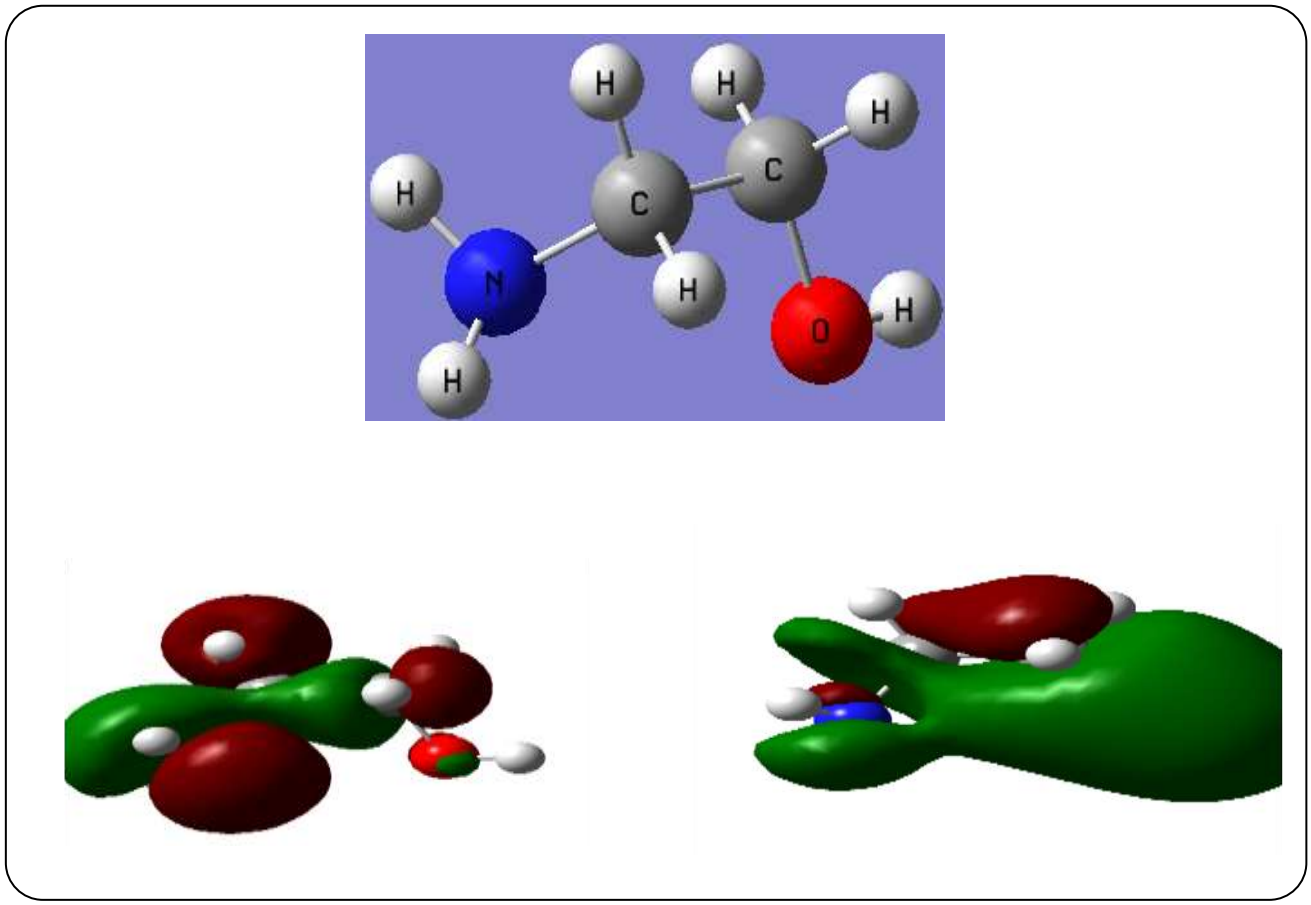

Fig. 10: Optimized structure of the studied molecule obtained by B3LYP-6-31 G(d) method ,and frontier molecular orbital of ETA.

B3LYP-6-31 G(d) method ,and frontier molecular orbital of ETA is represented in Fig. 10.

SEM analysis

The surface morphology of copper specimens, immersed in 100 ppm NaCl solution for 240h at 298 K without and with 0.4 vol % ETA inhibitor, are examined by scanning electron microscopy (Fig.11). In the absence of ETA, The sample surface is corroded (Fig.11a); whereas in its presence, the sample surface (Fig.11b) is well protected and the micrograph shows the protected film morphology. These results indicate that copper corrosion in 100 ppm NaCl solution is inhibited significantly by ETA.

CONCLUSIONS

Electrochemical study results demonstrate that ETA film effectively inhibits copper from corrosion in 100 ppm NaCl solution .The inhibition efficiency could be up to 99, 78% at 0.4 vol % ETA.

Potentiodynamic polarization studies show that ETA molecules act as a mixed –type inhibitor. The ETA adsorption on copper surface, in sodium chloride solution, obeys to Langmuir adsorption isotherm model.

The electronic parameters: energy E_{HOMO} of molecular orbitals, energy E_{LUMO} of atomic orbitals, ΔE energy gap, dipole moment and total energy indicate that the inhibitor molecules' adsorption on copper surface is stable and therefore effective.

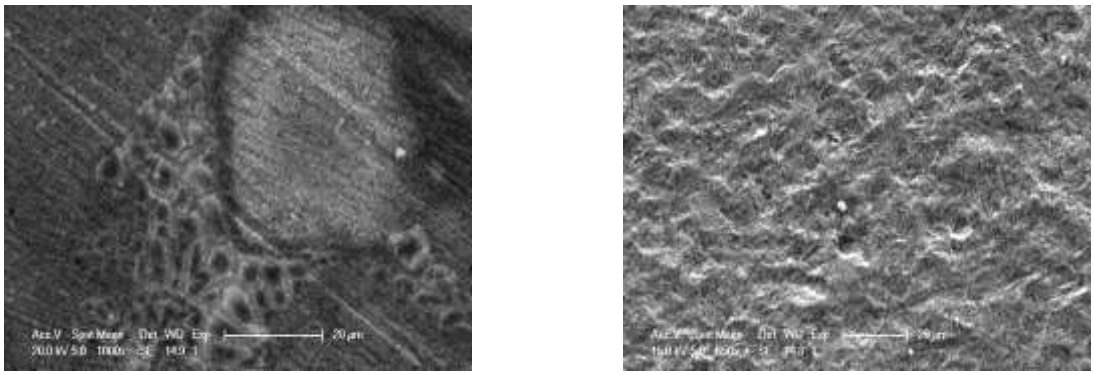

(a) (b)

Fig. 11: SEM micrographs of copper surfaces (a) without inhibitor, (b) with inhibitor immersed in 100 ppm NaCl solution for 240h at 298K.

SEM results clearly indicate that copper corrosion can be inhibited by ETA adsorption on copper surface.

Acknowledgement

The authors thank Mrs. Nora Zennadi for helping with translation work.

Received : Aug. 13, 2015 ; Accepted : Feb. 15, 2016

REFERENCES

[1] Qudah -M.A.Al, Inhibition of copper corrosion by flavonoids in nitric acid, *E-Journal of Chemistry*, **8**(1): 326-332 (2011).

[2] Crousier J., Pardessus L., Crousier J.P., Voltammetry Study of Copper in Chloride Solution, *Electrochim. Acta*, **33** (8): 1039-1042 (1988).

[3] Kabasakaloglu.M, Kıyak.T, Şendil.O, Asan. A, Electrochemical Behavior of Brass in 0.1 M NaCl, *Applied Surface Science*, **193** (1-4): 167-174 (2002).

[**4**] Wang. C, Chen.S, Zhao. S, Inhibition Effect of AC-Treated, Mixed Self-Assembled Film of Phenylthiourea and 1-Dodecanethiol on Copper Corrosion, *J. Electrochem. Soc*, **151**(1): B11-B15 (2004).

[5] Khaled .K.F, Studies of the Corrosion Inhibition of Copper in Sodium Chloride Solutions Using Chemical and Electrochemical Measurements, *Mater. Chem. Phys.*, **125**: 427-433(2011).

[6] Hammouti B., Dafali A., Touzani R., Bouachrine M., Inhibition of Copper Corrosion by Bipyrazole Compound in Aerated 3% NaCl, *J. Saudi. Chem. Soc.*, **16:** 413-418 (2012).

[7] Li W., Hu L., Zhang S., Hou B., Effects of Two Fungicides on the Corrosion Resistance of Copper in 3.5 NaCl Solution under Various Conditions, *Corros.Sci.*, **53**: 735-745 (2011).

[8] Sudheer, Quraishi M.A., Electrochemical and Theoretical Investigation of Triazole Derivates on Corrosion Inhibition Behaviour of Copper in Hydrochloric Acid Medium, *Corros.Sci.*, **70**: 161-169 (2013).

[9] Gardiner .D.J, Gorvin A.C., Gutteridge C., Jackson A.R.W., Raper E.S., In Situ Characterization of Corrosion Inhibition Complexes on Copper Surfaces Using Raman Microscopy, *Corros. Sci.*, **25**: 1019-1027 (1985).

[10] Sherif E.M., Park S.M., Inhibition of Copper Corrosion in Acidic Pickling Solutions by N-phenyl-1,4-phenylenediamine, *Electrochim. Acta*, **51**: 4665-4673 (2006).

[11] Khaled K.F., Experimental and Atomistic Simulation Studies of Corrosion Inhibition of Copper by A New Benzotriazole Derivative in Acid Medium, *Electrochim .Acta* , **54**(18**)**:4345-4352 (2009).

[12] Yan C.W., Lin H.C., Cao C.N., Investigation of Inhibition of 2-mercaptobenzoxazole for Copper Corrosion,*Electrochim.Acta*,**45**:2815-2821 (2000).

[13] Solmaz R., Ece Altunbas S., Ali D., Gùlfeza K., The Investigation of Synergistic Inhibition Effect of Rhodanine and Iodide Ion on the Corrosion of Copper in Sulphuric Acid Solution, *Corros. Sci.*, **53**: 3231- 3240 (2011).

[14] Zhang D.Q., An Z.X., Pan Q.Y., Gao L.X., Zhou G.D., Comparative Study of Bis-Piperidiniummethyl Urea and Mono-Piperi diniummethyl-Urea as Volatile Corrosion Inhibitors for Mild Steel, *Corro.Sci.*, **48**(6):1437-1448(2006).

[15] Ali E., Mohammad G., Reza M., Hossein M., Javad S., Electrochemical and DFT Study on the Inhibition of 316L Stainless Steel Corrosion in Acidic Medium by 1-(4-nitrophenyl)-5-amino-1H-tetrazole, *RSC.Adv*,**4**, p.2031-2037 (2014).

[16] Kertit .S , Hammouti. B, Corrosion Inhibition of Iron in 1M HCl by 1-phenyl-5-mercapto- 1,2,3,4- tetrazole, *Appl.Surf.Sci.*, **93**, 59-66 (1996).

[17] Larabi L., Benali O., Mekelleche S.M., Harek Y., 2-mercapto-1-methylimidazole as Corrosion Inhibitors for Copper in Hydrochloric Acid, *Applied Surface Science*, **253**(3) , p.1371-1378 (2006).

[18] Barouni K., Bazzi L., Salghi R. Mihit .M., Hammouti B, Albourine A., El Issami S., Some Amino Acids as Corrosion Inhibitors for Copper in Nitric Acid Solution, *Materials Letters*, **62**, 3325-3327 (2008).

[19] Avci G., Inhibitor Effect of N,N-Methylenediacrylamide on Corrosion Behavior of Mild Steel in 0.5 M HCl, *Mater.Chem.Phys*., **112**, 234- 238 (2008).

[20] Ali E., Reza M., Ahmad K., A.Y-F, Inhibitory of Newly Synthesized 3-BrPhOXTs on Corrosion of Stainless Steel in Acidic Medium, *S. Afr. J. Chem.*, **67**: 198-202 (2014).

[21] Ma H., Chen S., Niu L., Zhao S., Li S., Li D., Inhibition of Copper Corrosion by Several Schiff Bases in Aerated Halide Solutions, *Journal of Applied Electrochemistry*, **32**: 65-72 (2002).

[22] Ahamad I., Prasad Quraishi R.M.A., Inhibition of Mild Steel Corrosion in Acid Solution by Pheniramine Drug: Experimental and Theoretical Study, *Corros. Sci*., **52**: 3033-3041(2010).

[23] Ali E., Reza M., Maliheh A., Electrochemical Investigation of Inhibitory of New Synthesized 3-(4-Iodophenyl)- 2 Imino-2,3-Dihydrobenzo[d] Oxazol5-yl4-Methyl-benzensulfonate on corrosion of Stainless Steel in Acidic Medium, *J. Electrochem. Sci. Technol*., **6** (1): 7-15 (2015).

-